Recent developments in carbon nanotube membranes for water purification and gas separation

Sears, Kallista, Dumee, Ludovic, Schütz, Jürg, She, Mary, Huynh, Chi, Hawkins, Stephen, Duke, Mikel and Gray, Stephen (2010) Recent developments in carbon nanotube membranes for water purification and gas separation. Materials, 3 (1). pp. 127-149. ISSN 1996-1944

Materials **2009**, *2*, 1-x manuscripts; doi:10.3390/ma20x000x

OPEN ACCESS

materials

ISSN 1996-1944

www.mdpi.com/journal/materials

Review

Recent Developments in Carbon Nanotube Membranes for Filtration and Water Purification

Kallista Sears[1*], Ludovic Dumée[1,2], Jürg Schütz[1], Mary She[3], Mikel Duke[2] and Stephen Gray[2]

[1] CSIRO Materials Science and Engineering, Bayview Ave, Clayton Vic 3168, Australia;
[2] Institute for Sustainability and Innovation, Victoria University Werribee Campus, Hoppers Lane, Werribee PO Box 14428, Melbourne, Victoria, 8001, Australia
[3] Centre for Material and Fibre Innovation, Institute for Technology and Research Innovation, Deakin University, Geelong Vic 3217, Australia

* Author to whom correspondence should be addressed; E-Mails: kallista.sears@csiro.au; Tel.: +61-(0)3-95452105; Fax: +61-(0)3-95452363

Received: / Accepted: / Published:

Abstract: Carbon nanotubes (CNTs) are nanoscale cylinders of graphene with exceptional properties such as high mechanical strength, high aspect ratios and large specific surface area. To exploit these properties for membranes, macroscopic structures need to be designed with controlled porosity and pore size. This manuscript reviews recent progress on two such structures: (i) CNT Bucky-papers, a non-woven, paper like structure of randomly entangled CNTs, and (ii) isoporous CNT membranes, where the hollow CNT interior acts as a membrane pore. The construction of these two types of membranes will be discussed, characterization and permeance results presented, and some promising applications discussed.

Keywords: Carbon Nanotube, Bucky-paper, Membrane, Filtration

---

1. Introduction

Many water and gas purification techniques, such as membrane distillation and reverse osmosis, are reliant on membranes. Consequently, the development of advanced membrane technologies with controlled geometries and porosity is an important aspect for efficient and cost effective purification. Present polymeric membranes are well known to suffer from a trade off between selectivity and permeability, and in some cases are also susceptible to fouling or exhibit low chemical resistance.

Membranes based on carbon nanotubes (CNTs) offer a possible route to overcome these shortcomings with a number of interesting structures emerging [1-12]. CNTs are nanoscale cylinders of rolled graphene and can be capped at one or both ends with a half fullerene (Figure 1) [13]. They can be single walled (SWNT) or multi-walled (MWNTs) depending on the number of concentric graphene cylinders. CNTs exhibit remarkable electrical and thermal conductivity, and are one of the strongest fibers known [14,15]. These properties, combined with their nanoscale dimensions, have led to their intense study for a wide range of applications [16]. However fabricating macroscopic structures which have controlled geometries, porosity and pore shape, is still challenging.

This paper reviews two types of CNT macroscopic structures under consideration for membrane applications: (i) Bucky-paper membranes and (ii) isoporous CNT membranes. These two types of CNT membranes are distinctively different in their structure and arrangement of the CNTs. In the case of a Bucky-paper, the CNTs are randomly arranged into a non-woven, paper-like structure. This creates a highly porous membrane with a large specific surface area. In contrast the isoporous CNT membranes aim to use aligned CNTs as cylindrical pores across an otherwise impermeable membrane. As such it consists of nano-sized pores with a narrowly defined diameter, which are of interest for high-selectivity, high permeability nano-filtration applications. This paper reviews the various techniques used to fabricate these two types of CNT membranes and the associated challenges. It also discusses how the processing steps affect the final membrane structure and porosity and their possible uses for water and/or gas separation.

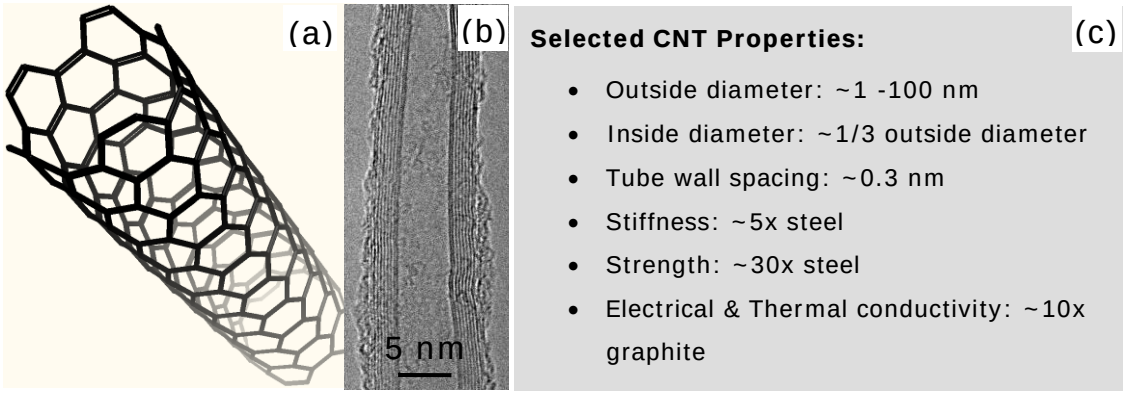

Figure 1 (a) Schematic of a carbon nanotube, (b) TEM image of a carbon nanotube showing a number of concentric walls, and (c) a list of selected CNT properties.

2. Bucky-Paper Membranes

The term "Bucky-paper" is used to describe a mat of randomly entangled CNTs prepared by filtration (Figure 2) [17] or an alternative papermaking process [18]. CNTs are known to have a strong tendency to aggregate due to Van der Waals interactions, and it is these Van der Waals interactions which also hold the CNTs together into a cohesive Bucky-paper. Due to the simplicity of their preparation, Bucky-papers were one of the first macroscopic structures fabricated from CNTs and their mechanical, electrical and thermal properties have been extensively studied [12,17,19-23].

2.1. Bucky-Paper Processing

Bucky-papers are typically formed by first purifying the CNTs and then dispersing them in a suitable solvent. Once a well dispersed solution is achieved, it is filtered through a porous support which captures the CNTs to form an optically opaque Bucky-paper (Figure 2). If the Bucky-paper is thick enough it can be peeled off the support filter intact. As shown by the origami plane in Figure 2c, Bucky-papers can be mechanically robust and flexible. Typically longer, narrower and more pure nanotubes lead to stronger Bucky-papers with higher tensile strengths [17,20,24].

As grown CNTs are highly entangled and typically contaminated with metallic catalyst particles and carbonaceous material such as amorphous carbon, fullerenes, and graphitic nano-particles. Consequently their purification and dispersion is a critical step in Bucky-paper processing and can affect both the Bucky-paper structure and properties [25-27]. Figure 3, for example, compares SEM images of Bucky-papers processed from a poorly dispersed and well dispersed CNT solution.

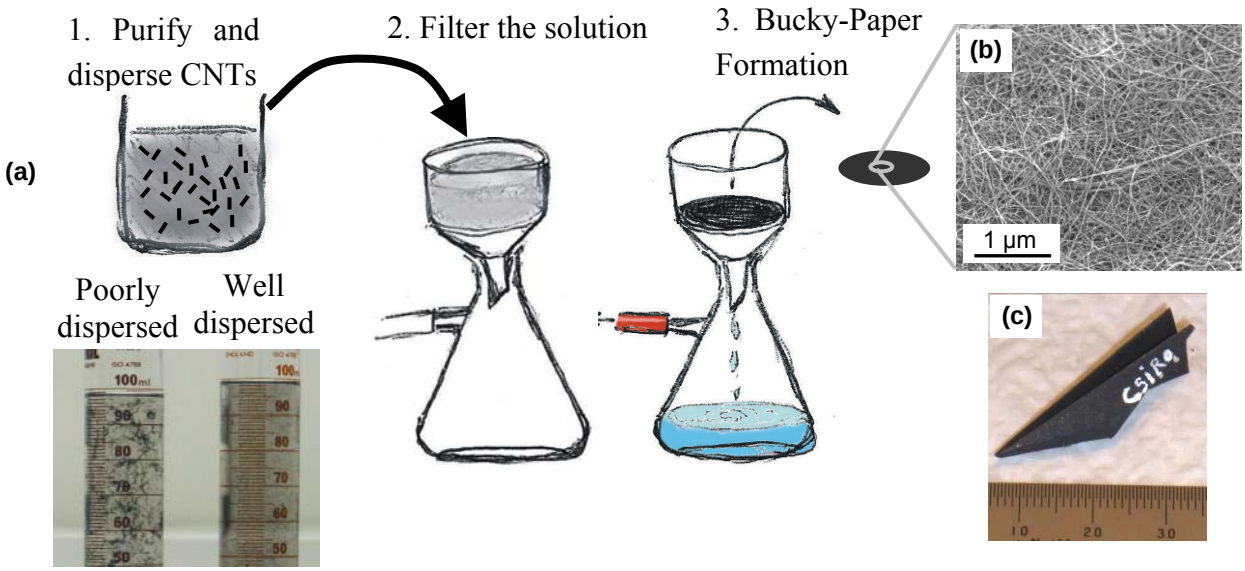

Figure 2. (a) Process for manufacturing Bucky-papers, (b) SEM image showing the Bucky-paper surface and (c) Bucky-paper origami aeroplane demonstrating their flexibility mechanical robustness.

For purification an oxidative treatment such as nitric acid (HNO_3) or annealing is commonly used to remove amorphous carbon which is oxidised more quickly than the CNTs. This is often followed by an acid treatment such as Hydrochloric acid (HCl) to dissolve any metal particles [24,28,28-30]. However these treatments can also damage and shorten the CNTs as well as functionalise them with carboxyl and hydroxyl groups [31,32]. This can be advantageous for dispersion into polar solvents such as water. However it can also alter the natural CNT properties. The chemical purification steps can also be combined with physical processes such as filtration and centrifugation [28,33]. For CNT dispersion a combination of the following strategies are typically used[34,35]:

(i) covalent functionalization of the CNT surface to improve their chemical compatibility with the dispersing medium [36,37].

(ii) the use of a third component such as a surfactant [34,35,38-40], polymer [41] or biomolecules (such as DNA [42]).

(iii) mechanical treatments such as ultrasonication and shear mixing.

The purification and dispersion steps need to be carefully chosen to suit the type of CNTs, the impurities that are present, and the final application so that the desired CNT properties are not adversely affected [24,43]. Further details on purification and dispersion techniques can be found in a number of articles and reviews [34]

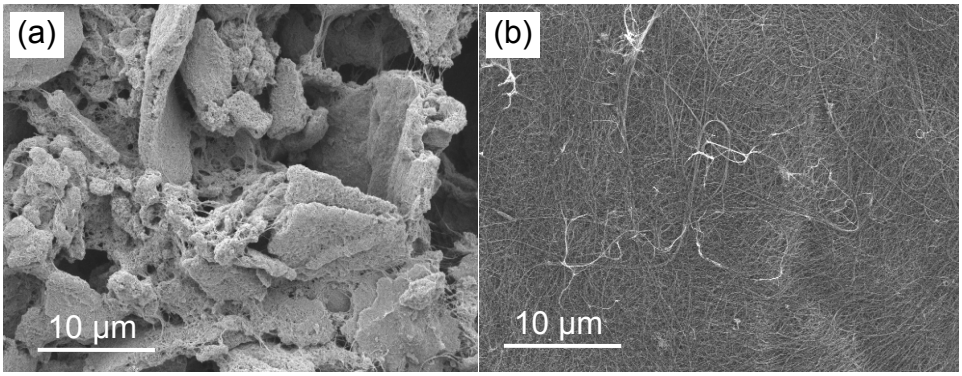

Figure 3. SEM image showing the surface of a Bucky-paper formed from (a) poorly dispersed single walled carbon nanotubes and (b) well dispersed CNTs (2 keV, 5 mm working distance). [24,37,43]

2.2 Bucky-paper Structure and Properties

As illustrated in Figure 2b, Bucky-papers tend to form a highly porous network of randomly orientated CNTs. The high porosity and random CNT arrangement are particularly evident in movie S1 (supplementary information) which shows a series of TEM images taken with increasing sample tilt from 30 to 150°. Clearly Bucky-paper membranes do not consist of well defined pores of a single characteristic shape and size. Instead the voids between the entangled CNTs form a highly porous 3D network. Despite this, SEM imaging of the surface followed by image analysis, is useful for calculating an "apparent surface" pore size as shown by the histogram and inset of Figure 4 [12,44,45]. The analysis shown in Figure 2b or 3b of 4? is for a Bucky-paper fabricated from MWNTs grown by

chemical vapour deposition (CVD) that have an average outer diameter and length of 9 nm and ~300 µm, respectively (see Table 1–fine CNTs). The CNTs were dispersed in analytical grade isopropanol by sonication and stirring, and then immediately filtered though a poly(ether-sulfone) (PES) support of 0.45 µm pore size. No acid treatments or purification steps were used in order to preserve their inherent hydrophobicity (see section 2.3.1). The resulting structure was nevertheless of a high purity (>95% CNT) due to careful choosechoice of the CVD growth technique and parameters. While the average pore size is quite small (~25 nm), the pore size distribution is significantly quite broader with pores of up to 105 nm mean diameter. This is consistent with pore size distributions reported by other groups for similar MWNTs [46-48], where the average pore size was ??nm and the larger pore sizes were ??nm. Figure 4 (stars/right axis) also shows results from particle (polystyrene) rejection tests for the same Bucky-paper. These are in reasonable agreement with a rejection of 80% for 100 nm diameter spheres and 98% for 500 nm diameter spheres[.2].

The Bucky-paper pore size is also highly dependent on the type of CNTs used. Figure 5 illustrates how this can be used to tune the average pore size by mixing two types of CNTs in different ratios. The two types of CNTs are referred to as fine (~9 nm outer diameter) and coarse (~37 nm outer diameter) with reference to their outer diameter and other structural properties (Table 1 and Figure 5b-c). Bucky-papers formed solely from fine or coarse CNTs had an average surface apparent pore size of ~20 and 49 nm, respectively, while intermediate pore sizes were obtained for mixtures of the two (Figure 5). Other groups have shown ways to control porosity and pore size via other techniques. Kukovecz et al., for instance, have varied the Bucky-paper pore size via the length of their CNTs, which was varied from 2 µm down to 230 nm length through a ball milling treatment [47]. Das et al. controlled the porosity by dispersing polymer beads together with the CNTs to form a PS/CNT Bucky-paper composite [49]. The polymer beads were subsequently dissolved creating voids in the Bucky-paper. Figure 6 shows surface and cross-sectional SEM images of a similar composite structure formed by our group using polystyrene beads from Sigma Aldrich (L1528).

Bucky-papers also offer incredible porosity and specific surface area. Helium pycnometer measurements made on Bucky-papers fabricated from the fine and coarse CNTs discussed earlier, indicated porosities of 91% and 87%, respectively. Furthermore Cinke et al. reported a specific surface area as high as 1587 m^2/g for Bucky-papers formed from SWNTs [28]. They attributed this high surface area to their two step purification process which ensures that the CNTs are de-bundled and highly pure. Figure 7 plots specific surface areas (based on N_2 adsorption isotherms) taken from the literature as a function of the CNT outer diameter. As expected a monotonic decrease in the specific surface area is observed with increasing diameter. Since nitrogen cannot penetrate into the space between concentric graphitic walls of MWNTs, the specific surface area to CNT mass decreases with increasing CNT diameter. The data points represented by open circles in Figure 7 are from CNT samples for which a high content of impurities had been reported. Judging from the significantly lower surface areas that have been measured for these samples it seems plausible that the specific surface area is higher after impurities have been removed.

Several authors have investigated methods to introduce CNT alignment in Bucky-papers (Figure 8) [50,51]. Their results indicated enhanced conductivity along the alignment direction and that the porosity and pore structure is also likely to be affected [52,53].

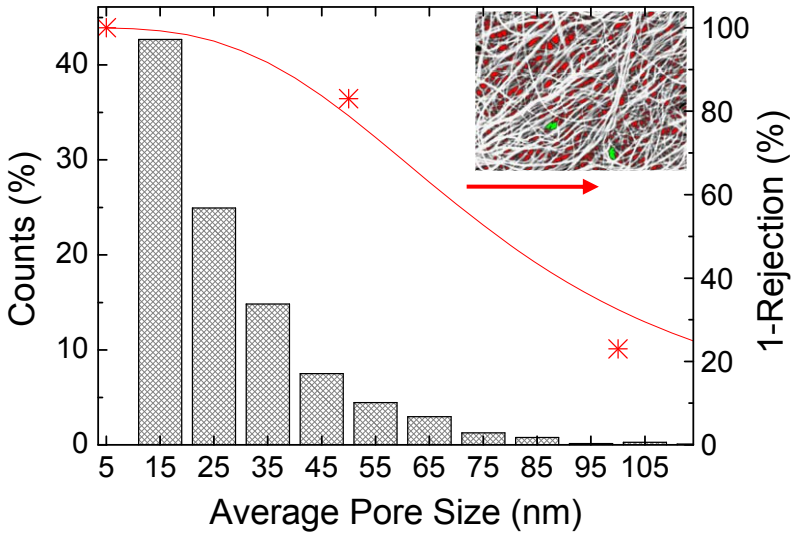

Figure 4. (Histogram - left axis): Average pore size distribution determined by SEM imaging of a Bucky-paper. (Red stars – right axis): Particle rejection tests with polystyrene spheres. The Bucky-paper was formed by dispersing "fine" carbon nanotubes grown by chemical vapor deposition in isopropanol using sonication. The as grown nanotubes had an impurity content of <5% and did not undergo further treatment in order to maintain their natural hydrophobicity.

Table 1. Properties of the coarse and fine carbon nanotubes grown by CVD.

CNT Type	***Coarse***	***Fine***
Inner diameter (nm)	10 ± 5.5	4.5 ± 1
Outer diameter (nm)	37 ± 16	9 ± 1.5
# walls	37 ± 21	6 ± 2
Impurity content	<10 wt%	<2 wt%

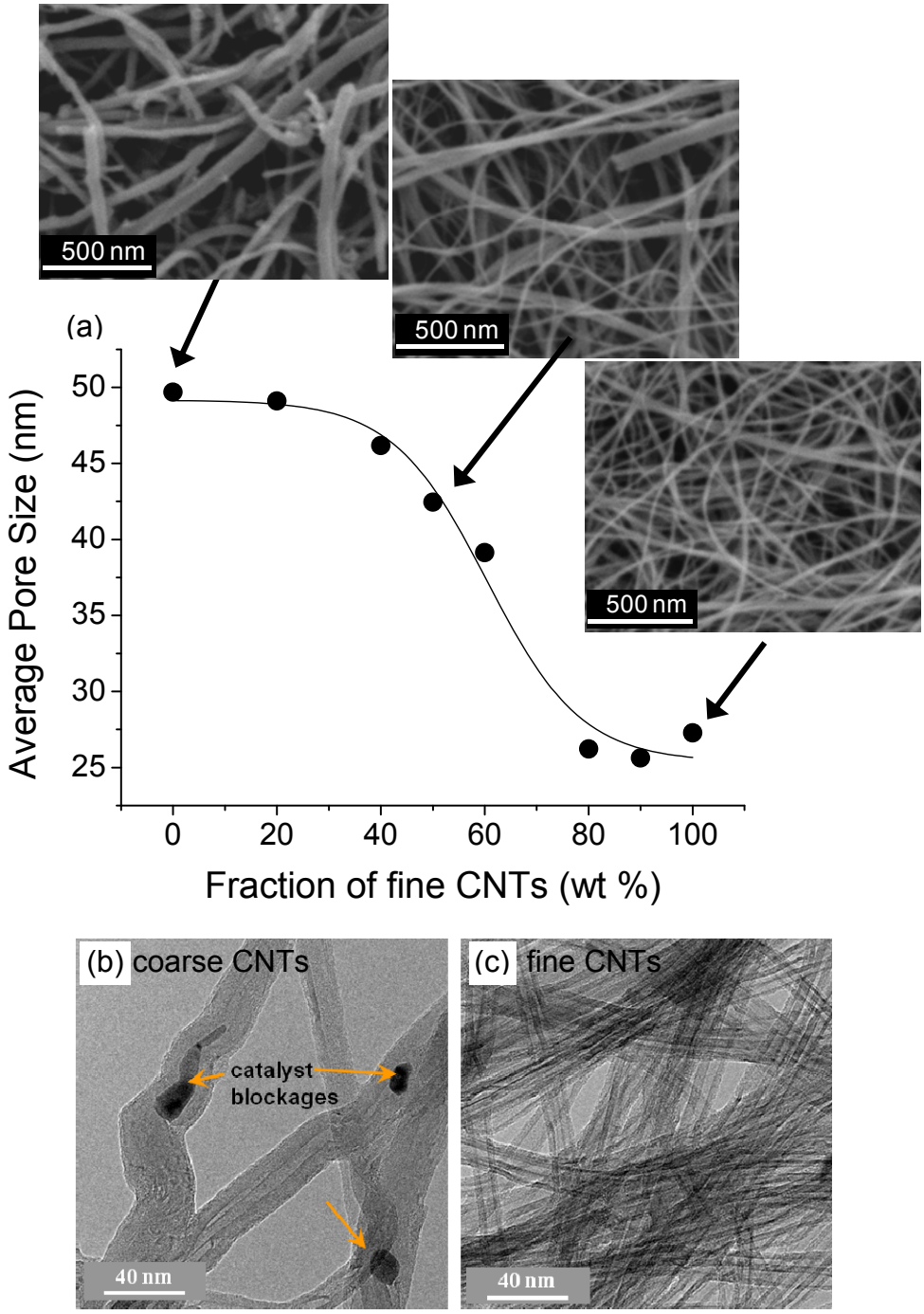

Figure 5. (a) Dependence of the Bucky-paper pore size on the ratio of "fine and coarse" carbon nanotubes. The SEM images show the Bucky-paper surface for three compositions as indicated. (b) and (c) are TEM images (200kV) of the coarse and fine nanotubes, respectively. The CNT properties are also summaries in Table 1. The nanotubes were dispersed by sonication in isoproanol and did not undergo purification processes.

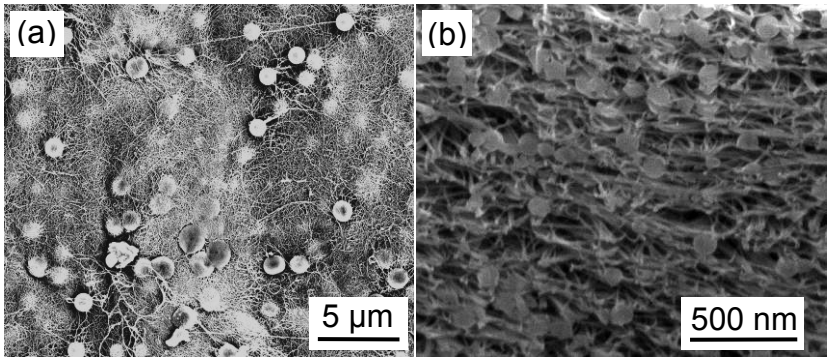

Figure 6. SEM images showing (a) the surface and (b) a cross section (52° sample tilt) of a Bucky-paper formed from a mixed dispersion of PS beads and multi-walled carbon nanotubes (5 keV, 5 mm working distance). The PS beads in (a) and (b) had 1 μm and 100 nm diameters, respectively. The cross-section was formed by milling with a Ga Focused Ion Beam.

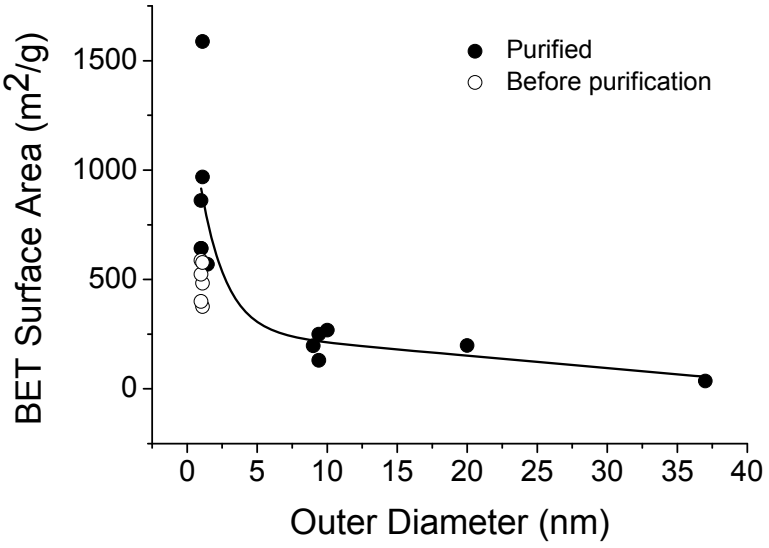

Figure 7. Dependence of carbon nanotube surface area on nanotube outer diameter. The data was taken from the literature and our own measurements (see Table S1, supplementary materials for further details and references for the data). The open circles represent results for nanotubes reported to have high impurity content.

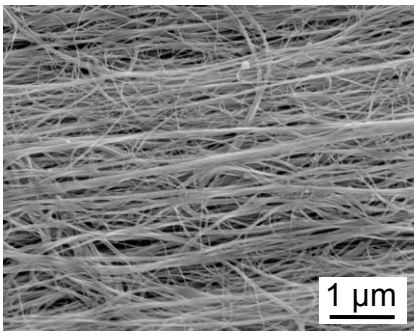

Figure 8. SEM image showing the surface of an aligned carbon nanotube "Bucky-paper" (5 keV, 5 mm working distance).

2.3 Bucky-Papers for Water Purification and Filtration

2.3.1 Membrane Distillation

In terms of the application of Bucky-papers, the authors' work with Bucky-paper membranes concentrates on their use for water purification by a process called direct contact membrane distillation. This technique is an alternative to reverse osmosis and other desalination techniques, particularly when the concentration of solutes is high [54]. As illustrated in Figure 9, the Bucky-paper is used as a highly hydrophobic membrane to separate a feed of hot sea or brackish water from a permeate of cold fresh water. While liquid cannot cross the air gap formed by the membrane, water vapor is able to pass through the pores from the hot feed to the cold permeate driven by the difference in partial vapor pressure. This vapor then condenses on the permeate side creating fresh water. The inherent hydrophobicity of the nanotubes (D.I. water contact angle ~113°) and high Bucky-paper porosity (~90%) lend them to this application and we have demonstrated water vapor permeabilities of up to 3.3×10^{-12} kg/m^{2}sPa on a small scale rig [12,44]. However, cracking of the Bucky papers with time [?] is a problem, as brine is able to penetrate the relatively large cracks leading to brine breaching of the Bucky-paper and a decrease in permeate quality [?]. Figure 10 demonstrates how the vapor flux increases with the difference in partial vapor pressure across the membrane. The two curves in Figure 10 represent results from a pure Bucky-paper (solid circles) and from a composite Bucky-paper (open circles). The composite Bucky-paper was created by vacuum filtering a solution of PVDF through the Bucky-paper structure in an attempt to decrease cracking of the Bucky papers and to extend their useful lifetime in this application. In this process the PVDF forms a thin coating on the CNTs which increases the membrane mechanical robustness and operational lifespan. This however comes at the expense of a lower porosity and hence reduced flux and permeability [44].

2.3.2 Other Applications

Several groups have demonstrated desalination of low salinity (<??)[.3] water using Bucky-paper like structures in a Capacitive De-Ionization setup [55-59]. This application takes advantage of the electrical conductivity and high porosity offered by Bucky-papers. The setup comprises ~~of~~ two electrodes arranged to form a parallel plate capacitor across which a voltage is applied to absorb salt

ions of opposite polarity from a stream of salty water. The salt is then released as a concentrated brine when the applied potential is reversed. Wang et al. demonstrated an electrosorption capacity of ~57 μmol/g, which was similar to a carbon aerogel electrode despite its lower surface area and is attributed to the more optimal pore size distribution of the Bucky-paper [57].

Bucky-papers have also been used as fine filters. Viswanathan et al. reported that a 2 μm thick CNT Bucky-Paper film supported on a cellulose acetate disc was capable of filtering fine particles of 100-500 nm diameter to a level that exceeded the standards set out for HEPA filters [60]. They also suggest that these Bucky-Papers could be used to filter powdered organic dyes and condensed lead fumes.

Antimicrobial properties (in the absence of UV/vis irradiation) and the efficient bacterial removal from contaminated waters have also been demonstrated [4,61,62]. Brady-Esétvez et al. demonstrated that a SWNT Bucky-paper was effective in completely retaining E. coli cells (2 μm size) due to size exclusion and also promoted their inactivation [4,62]. They also demonstrated exceptionally high removal of the model virus MS2 bacteriophage (27 nm diameter) due to depth filtration.

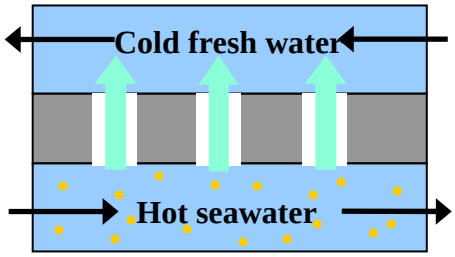

Figure 9. Principle behind Direct Contact Membrane Distillation

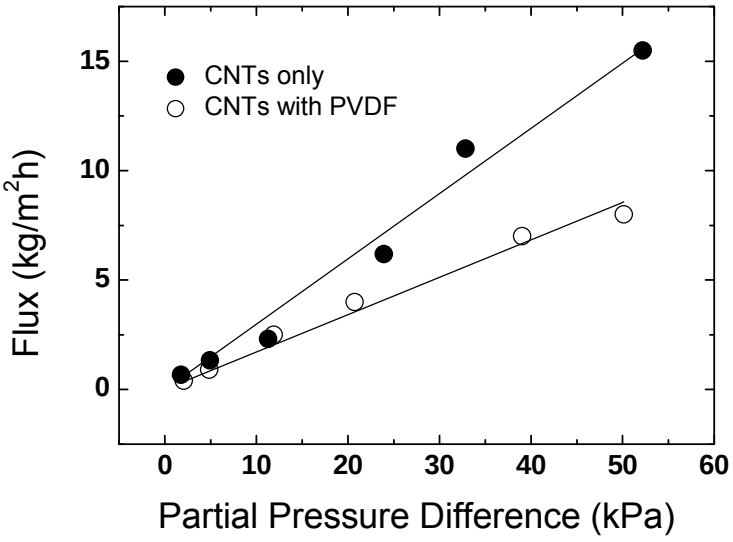

Figure 10. Dependence of water vapor flux on the partial pressure difference across a Bucky-paper membrane in a direct contact membrane distillation setup [stream flux 300 mL/min; salt concentration ~ 35g/L; T_{cold} ~ 5ºC , T_{hot} varied from 25 to 95ºC

3. Isoporous Carbon Nanotube Membranes

This structure is distinct from a Bucky-paper in that it uses the CNTs as cylindrical pores across an otherwise impermeable thin film (Figure 11c). This results in a membrane with well controlled nanoporosity with the only route for flow through the hollow CNT interior. These structures are promising for high permeability, high selectivity membranes due to the small nanotube diameter (as small as 0.7 nm) and predictions of rapid flux through their hollow interior [63-66]. Molecular dynamic simulations have also shown that CNT membranes, in theory, can be used for desalination via reverse osmosis [67].

The predicted rapid flux through CNTs is attributed to two factors. First and foremost is the CNT's smooth, frictionless interior. This is predicted to result in specular instead of diffusive collisions between molecules and the CNT wall, leading to enhanced flow for (i) gases in the Knudsen regime [4,64,65] and (ii) pressure driven liquid flow through a pipe (classically described by the Hagen-Poiseuille law) [68]. Secondly, for CNTs with diameters less than ~2 nm, molecular ordering and single file diffusion have been predicted to lead to the concerted movement of molecules and enhanced flow rates [63,66,67,69-72]. In particular Hummer et al. predicted ballistic motion of water chains through the CNT interior due to strong hydrogen bonding between water molecules and minimal interaction with the CNT wall [63].

While it is intuitively unfavorable for a polar molecule, such as water, to enter the non-polar interior of a CNT, experimental evidence has proved it possible [1-3,11,73-78]. One of the first demonstrations of liquid flow through a CNT was by Sun et al. who embedded an individual MWNT (inner diameter 150 nm) into an epofix epoxy resin followed by microtoming to form thin membrane slices [74]. However it was the work of two separate groups, Hinds et al and Holt et al., that caught the interest of the scientific community [1-3]. Both groups independently fabricated membranes with a high density of aligned CNT pores and demonstrated fluid flow 2-3 orders of magnitude greater than that predicted by conventional fluid flow theory, although their results have been questioned [68]. Both of these groups have also reported functionalization of the CNT tips to gate fluid flow through the CNT pores or enhance their selectivity [79-83]. Since these findings, a number of groups have reported on the construction and permeance of isoporous CNT membranes (Table S2). In the following sections the different approaches to membrane construction will be reviewed. While Holt and Hinds are still the only two groups to have reported water flow through the interior of CNT pores, a number of groups have reported permeance for gases. Consequently gas permeance is a useful

parameter by which to compare the various approaches to membrane construction and is presented in section 3.2.

3.1 Membrane Construction

For membrane construction, most groups use variations on the general approach outlined in Figure 11 [1,2]. Construction typically begins with a forest of aligned CNTs grown by Chemical Vapor Deposition (CVD) on either a silicon or quartz substrate (Figure 12). The spaces between the CNTs are then infiltrated with an impermeable material to form a continuous matrix. The excess matrix material and substrate are then removed opening up the ends of the CNT's.

In our method we form a matrix by infiltrating the CNT forest with a two part, low viscosity epoxy followed by curing at an 80-120°C [84]. Most importantly, the matrix needs to be void free, while at the same time preserving the CNT alignment. Figure 13 shows SEM and TEM images of one of our CNT forests after embedding with epoxy. Clearly, the epoxy conforms well to the CNTs without any obvious cracks or voids. Due to surface tension effects during infiltration, the CNTs are densified into columns (bright contrast) creating CNT free regions in between (Figure 13a). However the forest height before and after infiltration remains the same indicating that the CNT alignment is largely maintained. To further investigate the degree of CNT alignment, Raman spectra were measured for an as grown forest and an epoxy infiltrated one (Figure 14). The Raman intensity is sensitive to the CNT alignment and is strongest for incident light polarized parallel to the CNT axis [85-87]. A qualitative measure of the CNT alignment is therefore possible by measuring the intensity ratio, $I_{\parallel}/I_{\perp}$, between parallel and perpendicularly polarized light. Values of 3 and 2 were determined for the as grown and epoxy infiltrated forests respectively, indicating some loss of alignment. Vapor phase infiltration, such as that used by Holt et al., may better preserve the CNT alignment [1].

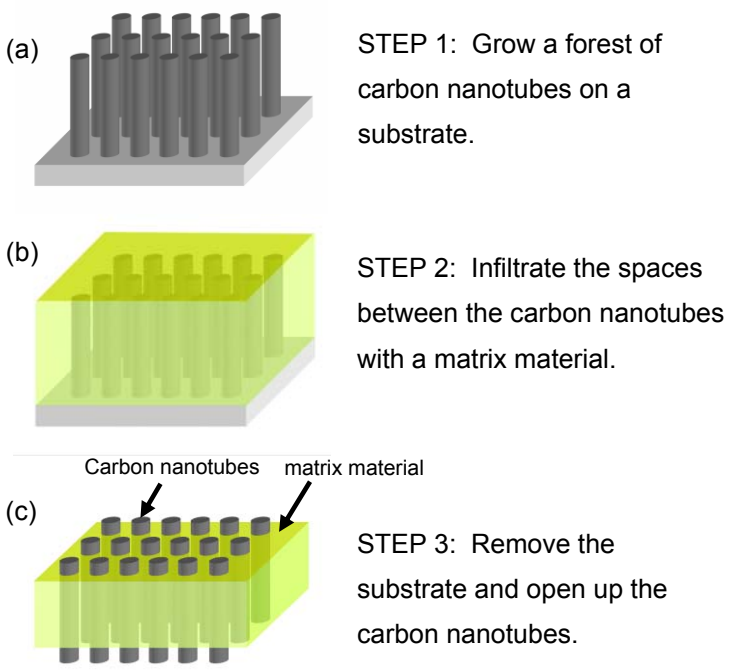

Figure 11. Schematic showing the basic steps used by Holt et al. and Hinds et al. to form "through tube" CNT membranes. The carbon nanotubes act as pores across an otherwise impermeable material [?, ?].

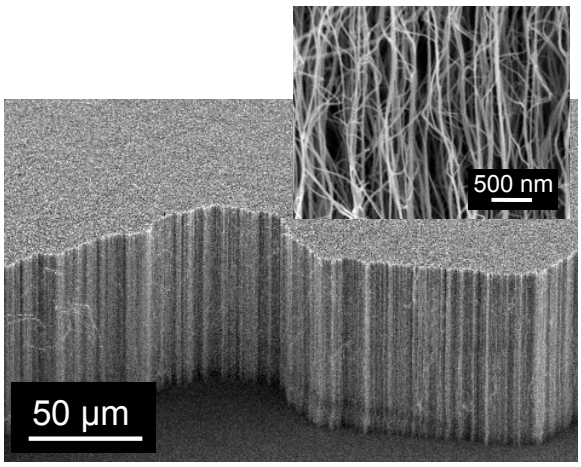

Figure 12. SEM image of a CNT forest grown by chemical vapor deposition on a silicon substrate. The inset shows a higher magnification image.

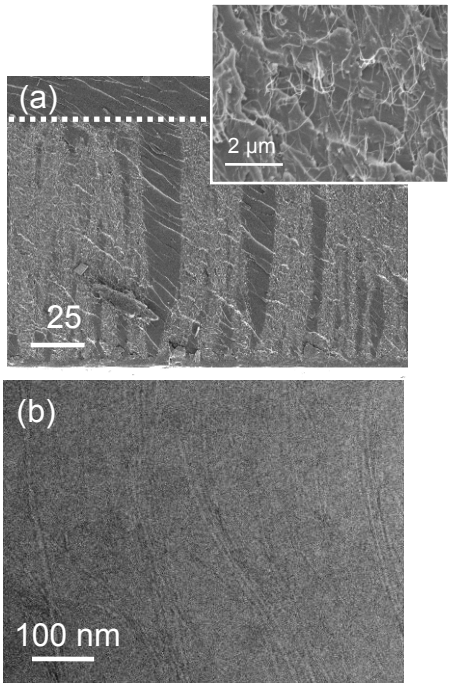

Figure 13. Images of a CNT forest after infiltrating with an epoxy (a) SEM image of a liquid nitrogen fractured cross-section. The CNTs are compacted slightly into columns (bright regions) due to surface tension effects, leaving CNT free regions (dark) in between. (b) TEM image (sample prepared by focus ion beam milling). The contrast between the CNTs and epoxy is low due to their similar carbon based composition.

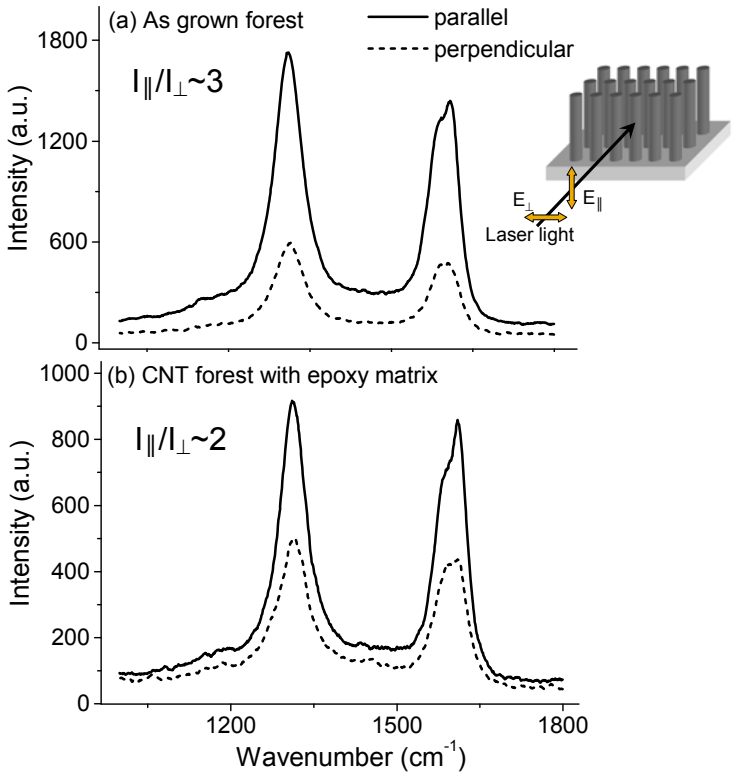

Figure 14. Raman spectra taken from (a) an as grown CNT forest and (b) a forest after infiltrating with epoxy. Both the D (1310 cm^{-1}) and G(1590 cm^{-1}) bands are present. The Raman signal intensity is sensitive to the CNT alignment and is strongest when the incident polarization is parallel to the CNT axis. It can therefore give an indication of the CNT alignment. A 783 nm laser with incident power of 2×10^4 W/cm^2 was used to avoid luminescence from the epoxy resin.

To remove the excess matrix material and open up the CNTs, polishing and/or oxygen based (H_2O or O_2) plasma treatments are commonly used [1,2,10]. Figure 15 shows SEM images of an epoxy infiltrated forest after first polishing with diamond paste and then plasma etching with an O_2/Ar mixture. Few CNTs (bright contrast) are visible after polishing, while many more are exposed by the plasma treatment (Figure 15b). Unfortunately CNT bundling and limited SEM resolution makes an accurate assessment of the number of exposed CNTs difficult. However, the increased number of exposed CNTs is reflected in the air permeance which increased by an order of magnitude from 5×10^{-15} to 4×10^{-14} moles/m/s/Pa. This is still an order of magnitude lower than that predicted by Knudsen diffusion if all of the CNTs in the as grown forest were open and spanning the membrane, and clearly indicates that the majority of CNTs are not yet open.

A number of groups have taken slightly different approaches to that outlined in Figure 11. Mi et al. grew the initial CNT forest directly onto a macroporous alumina substrate [10]. The alumina substrate acts as a support for the final CNT membrane and avoids the etching step required for non-porous silicon or quartz substrates. However it comes at the expense of a reduced CNT density which is reflected in the gas permeance discussed in Section 3.2.

Even at a typical forest density of 10^{11} cm^{-2} and CNT inner diameter of 5 nm, the total CNT areal coverage and hence porosity is less than 2%. To improve the available area for permeation, Yu et al. fabricated a dense block of aligned CNTs by shrinking an as grown CNT forest [88]. To shrink the forest they first detached it from the substrate by a water etching step and then collapsed it into a single block using the capillary forces generated by solvent evaporation [89,90]. Yu et al. did not apply a matrix material to the condensed forest so that fluid flow is possible through both the CNT interior and gaps between CNTs, which they estimated were less than 3 nm [88].

Kim et al. have reported on a scalable method of fabricating membranes which involves first dispersing amine-functionalized CNTs in tetrahydrofuran (THF) and filtering this solution through a porous PTFE substrate [6]. The CNTs appear to spontaneously align themselves perpendicular to the porous PTFE substrate in the draft of the fluid. These CNTs are then embedded in a polysulfone layer. Surprisingly, the polysulfone layer does not seem to block all of the CNTs as they report gas permeance without applying further surface treatments.

Finally, an approach used by several other groups is to grow CNTs within the pores of an anodized alumina template. This leads to forests of vertically aligned, straight CNTs within an alumina matrix. However it appears that these CNTs are only semi-graphitic. As such they do not possess the inherent smoothness and hydrophobicity of a purely graphitic CNT and may not exhibit the same fluid flow properties [11,73,91]{Velleman, Shapter, et al. 2009 #297}.

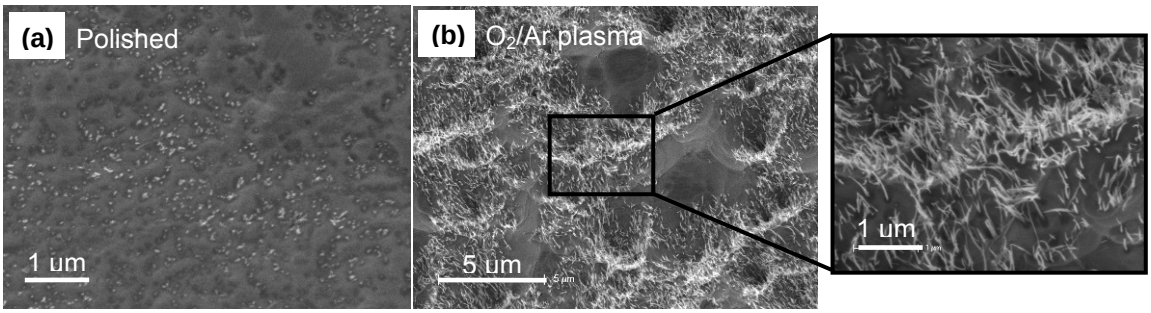

Figure 15. SEM images showing the CNT membrane surface after (a) polishing and (b) a 4 hour plasma treatment with a mixture of 30% O_2 in Argon. The plasma treatments were performed at a pressure of 0.6 mbar and power of 80W in a Diener Pico PC system [?].

3.2 Gas Permeance

The gas permeance reported by the various groups discussed above are compared in Table S2 and Figure 16a. Here, we define permeance as the flux through the membrane divided by the membrane area and the differential pressure. The membrane permeance is affected most by the CNT density. For example the highest permeance in Figure 16a is for the membrane reported by Yu et al. which was formed by densifying an as grown forest [88]. In contrast the membrane structure reported

by Mi et al. which was based on a low density CNT forest has a permeance 3 orders of magnitude lower[10]. Figure 16 also shows permeance results for three track etched polycarbonate (PC) membranes with 10, 15 and 30 nm pores. The 10 and 30 nm membranes were measured by the authors while the value for the 15 nm PC membrane was taken from the paper of Holt et al [1]. The PC membranes consist of well defined cylindrical pores and therefore offer an ideal benchmark for the CNT membranes. Interestingly, the gas permeance for CNT membranes reported by Yu, Holt and Kim are ~200, ~20 and ~2 times that of a commercial 10 nm PC membrane, respectively, despite their smaller pore diameter.

Figure 16b compares the enhancement factor for the same membranes and enables a more direct comparison by taking into account differences in membrane thickness, CNT diameter and CNT density. The enhancement factor is defined here as the experimental permeance (plotted in Figure 16a) divided by the permeance predicted from Knudsen theory. Knudsen diffusion applies when the mean free path divided by pore radius is greater than one, which is the case for all of the membranes reviewed here (see Table S2). In the Knudsen regime, there are more collisions with the CNT wall than with other molecules and the permeance, f_k [moles/m^2/s/Pa] is given by:

$$f_K = \frac{\varphi}{3}\sqrt{\frac{8}{\pi RTM}}\frac{1}{\tau L}\rho_{pores} \times A_{pore} \quad (1)$$

where φ is the CNT diameter [m], ρ_{pores} is the density of pores [m^{-2}], R is the universal gas constant [J moles^{-1} K^{-1}], T is the temperature [K], M is the gas molecular weight [kg/mole], L is the membrane thickness [m], τ is the pore tortuosity and A_{pore} is the inner area of each CNT [m^2] and is equal to $\pi \varphi^2/4$. The biggest uncertainty in determining the enhancement factor lies in an accurate knowledge of the density of CNTs that are open and spanning the membrane. Typically SEM or TEM imaging has been used to estimate an upper value [1,6,10].

The enhancement factor lies between 1-10 for most groups (Figure 16b) indicating reasonable agreement with Knudsen diffusion. The exception to this is Holt et al who reports an enhancement factor of ~60 [1]. This may be due to the small CNT diameter used (1.6 nm) and their sophisticated fabrication route which may ensure that a greater percentage of open CNTs. Interestingly the PC membranes show a similar if not slightly higher enhancement factor than the CNT membranes (with the exception of Holt et al.). This may be due to a non-uniform CNT diameter along the PC pores, or alternatively other transport mechanisms such as viscous flow may be contributing. However this indicates that the enhancement factor should be treated with caution, as it is highly dependent on the input values and an accurate value of CNT diameter and density.

Most reported studies found that the single-component selectivity exhibited the inverse-square-root scaling with molecular mass characteristic of Knudsen diffusion[1,6,10,88]. Holt et al. found that hydrocarbons were an exception to this and exhibited higher selectivities [1]. This was attributed to the preferential interaction of hydrocarbons with the CNT internal walls and possibly surface diffusion. Hence it may be possible to separate mixtures such as CO_2/CH_4 through this mechanism.

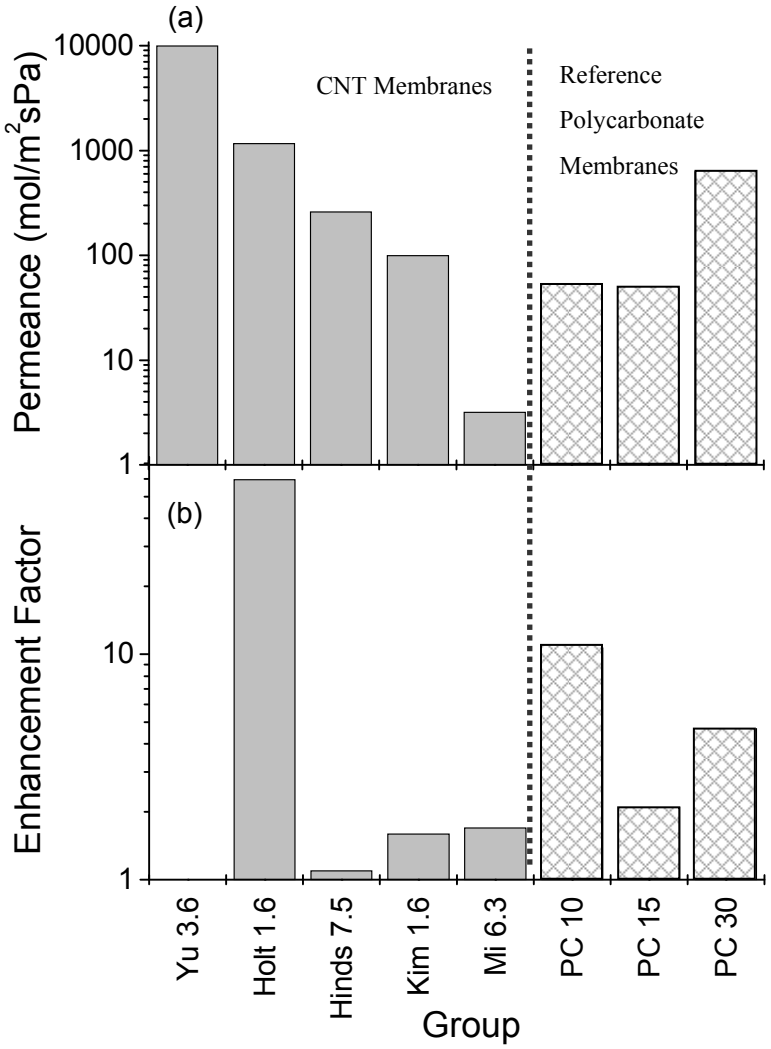

Figure 16. Summary of gas permeance values reported in the literature. (a) Permeance and (b) Enhancement Factor which is defined as the measured permeance divided by the permeance predicted by Knudsen theory. An enhancement value is not given for Yu, as flow is through both the CNT hollow interior and gaps between CNTs. The last three cross-hatched bars are for polycarbonate track etched membranes. These membranes also consist of well defined circular pores and therefore serve as an excellent benchmark to the CNT membranes. PC10 and PC 30 were measured by the authors, while PC15 is taken from {Holt}. The pore diameter (in nm) is given after the name of each group.

4. Conclusions

In summary this paper has reviewed the fabrication and application of two types of CNT based membranes (i) Bucky-papers and (ii) Isoporous CNT membranes. Both of these membranes have distinctively different structures and porosity. Bucky-paper membranes are a mat of randomly entangled CNTs fabricated by vacuum filtration. The Bucky-paper properties depend on the type of

CNT used and their pre-treatment (purification and dispersion). However, they typically offer a highly porous structure with large specific surface area. As such they are of interest for applications such as direct contact membrane distillation, capacitive de-ionization and filtration, especially of bacteria and viruses. In contrast, the isoporous CNT membrane uses the CNTs as pores across an otherwise impermeable matrix material. As such it aims to utilize the fast transport properties predicted through the hollow CNT interior, to fabricate high flux, high selectivity membranes. However, the construction of this type of membrane is highly complex with only a handful of publications. Only two groups have demonstrated water transport through these membranes, and have reported phenomenal flow rates 2-3 orders of magnitude greater than that predicted from conventional fluid flow theory. Clearly CNTs are a promising candidate for the fabrication of new and improved separation membranes.

Acknowledgements

We gratefully acknowledge Ms Chi Huynh and Dr Stephen Hawkins for the synthesis of high purity carbon nanotube forests by CVD. We also wish to acknowledge the expert advice and assistance of Dr John Ward and Mark Greaves on SEM, and Dr Sergey Rubanov and Dr Kenneth Goldie at Bio 21 for focused ion beam milling. We are also grateful to Dr Lingxue Kong at Deakin University for fruitful discussions, Chris Skourtis for allowing us to use an image of his aligned CNT ribbons, and Zongli Xie and Lisa Wong for their help with BET measurements.

Supplementary Information

Movie of Mary's TEM imaging
Two tables (see below)
Further Experimental details

- TEM, SEM, FIB
- refer to Ludo's MD papers for BET test, Bead rejection tests, porosity test, BP processing, image analysis
- Raman
- Plasma systems
- gas permeance

Table S1 Summary of N2 BET surface area results reported in the literature for carbon nanotubes.

Group	CNT Type	Synthesis	Treatments	Walls	Outer Diameter (nm)	Surface Area (g/m^2)	BP
Onyesták 2003[92]	MWNT	CVD	none	7	9.4 ± 3	130	No
			purified	7		250	
Smajda 2007[46]	MWNT	CVD	purified (95 wt% CNT)	22	15 - 25	197.7	Yes
Muramatsu 2005[93]	DWNT	CVD	purified (95 wt% CNT)	2	1.41,1.56	569	Yes
	SWNT	HiPco (Carbon Nano-technology)	Used as purchased	1	0.85 - 1.26	642	Yes
Cinke et al. 2002[28]	SWNT	HiPco	none (22 wt% Fe)	1	0.93 - 1.35	577	No
			Purified (< 0.4 wt% Fe)*	1		1587	
Inoue 1998[94]	MWNT	Hyperion Catalysis Int. Co.	no further purification	9	10	268	No
Cooper 2003[95]	SWNT	Laser ablation (Johnson Space Center)	purified 10.5 wt% impurity	1	?	350-450	BP
Eswaramoorthy 1999[96]	SWNT	Arc discharge	none	1	1.1	376	No
			HCl	1	1.1	483	No
			HNO3	1	1.1	429	No
Yang 2002[97,98]	SWNT	HiPco (Carbon Nano-technology)	no further purification	1	0.8-1.2	524	No
			HCl	1	0.8-1.2	587	No
			oxidation+HCl	1	0.8-1.2	861	No
CSIRO	MWNT	CVD	None (add impurity)	6	9	197	BP
	MWNT	CVD	None (add impurity)	37	37	36	BP

* Purification included an initial step to debundle the CNTs.

Table S2 Summary of CNT Membrane Properties, permeance and permeabilities taken from the literature.

Group	Matrix Material	Treatments	Thickness (μm)	Diameter (nm)	CNT Density (10^9 cm^{-2})	Test gas	Permeability (10^{-13} mol $m^{-1}s^{-1}Pa^{-1}$)	Permeance (10^{-8} mol $m^{-2}s^{-1}Pa^{-1}$)		Factor	Knudsen Number
								Measured	Knudsen[b]		
Mi[10]	Polystyrene	polish + HNO_3	10	6.3	1.87	N_2	3.2	3.2	1.9	1.7	10.3
Kim [6]	Polysulfone	amine – functionalized CNTs	0.6	1.6	70	He	6	100	64	1.6[c]	81.3
Hinds[2,3]	Polystyrene	PS+ H2O	5	7.5	60	N_2	100	260	233	1.1	8.7
Holt [1]	Si_3N_4	RIE	2.6	1.6	250	air	283	1170	19.6	59.7	40.6
	PC[a] control (15 nm)	N/A	6	15	0.6	air	29.5	49	16.8	2.1	4.3
Yu [88]	Densified forest only	Water etching	750	3.6±0.9	2900	N_2	751000	10000	8.98	1114.8	18.1
CSIRO	epoxy	None	35	4.5	50	air	0.05	0.015	6.5	-	14.4
	epoxy	polish + O_2/Ar plasma	35	4.5	50[d]	air	0.3	0.1	6.5	-	14.4
	PC[a] control (10 nm)	N/A	6	10	0.6	air	32.5	53.5	5.0	10.7	6.5
	PC[a] control (30 nm)	N/A	6	30	0.6	air	380	630	134	4.7	2.2

[a]PC = a polycarbonate track etched membrane.

[b]In calculating the theoretical permeance assuming Knudsen flow, the tortuosity was assumed to be 1, except in the cases of Hinds and Mi where tortuosity values of 1.1 and 1.26 were given respectively.

[c]Kim et. al report an enhancement factor ~2 times larger than that calculated by us.

[d]Assuming that all the as grown CNTs are open and spanning the CNT. (need to check this for the other groups)

References and Notes

1. Holt, J. K.; Park, H. G.; Wang, Y.; Staderman, M.; Artyukhin, A. B.; Grigoropoulos, C. P.; Noy, A.; Bakajin, O.,Fast Mass Transport Through Sub-2-Nanometer Carbon Nanotubes. *Science* 2006, 312, 1034-1037
2. Hinds, B. J. *et al.*,Aligned Multiwalled Carbon Nanotube Membranes. *Science* 2004, 303, 62-65
3. Majumder, M. *et al.*,Enhanced flow in carbon nanotubes. *Nature* 2005, 438, 44
4. Srivastava, A. *et al.*,Carbon Nanotube Filters. *Nature* 2004, 3, 610-614
5. Li, X.; Zhu, G.; Dordick, J. S.; Ajayan, P. M.,Compression-modulated tunable-pore carbon-nanotube membrane filters. *Small* 2007, 3, 595-599
6. Kim, S.; Jinschek, J. R.; Chen, H.; Sholl, D. S.; Marand, E.,Scalable fabrication of carbon nanotube/polymer nanocomposite membranes for high flux gas transport. *Nanoletters* 2007, 7, 2806-2811
7. Kim, S.; Pechar, T. W.; Marand, E.,Poly(imide siloxane) and carbon nanotube mixed matrix membranes for gas separation. *Desalination* 2006, 192, 330-339
8. Peng, F.; Pan, F.; Sun, H.; Lu, L.; Jiang, Z.,Novel nanocomposite pervaporation membranes composed of poly(vinyl alcohol) and chitosan-wrapped carbon nanotubes. *J. Membr. Sci.* 2007, 300, 13-19
9. Peng, F.; Hu, C.; Jiang, Z.,Novel poly(vinyl alcohol)/carbon nanotube hybrid membranes for pervaporation separation of benzene/cyclohexane mixtures. *J. Membr. Sci.* 2007, 297, 236-242
10. Mi, W.; Lin, Y. S.; Li, Y.,Vertically aligned carbon nanotube membranes on macroporous alumina supports. *J. Membr. Sci.* 2007, 304, 1-7
11. Whitby, M.; Cagnon, L.; Thanou, M.; Quirke, N.,Enhanced Fluid Flow through Nanoscale Carbon Pipes. *Nano Letters* 2008, 8, 2632-2637
12. Dumée, L. F.; Sears, K. S. J.; Finn, N.; Huynh, C.; Hawkins, S.; Duke, M.; Gray, S.,Characterisation and evaluation of carbon nanotube Bucky-paper membranes for direct contact membrane distillation . *J. Membr. Sci.* Submitted,
13. Iijima, S.,Helical microtubules of graphitic carbon. *Nature* 1991, 354, 56-58
14. O'Connell, M. J., Editor, *Carbon Nanotubes: Properties and Applications* (Taylor & Francis Group, 2006).
15. Dresselhaus, M. S. ; Dresselhaus, G.; Avouris, Ph., Editors, *Carbon Nanotubes: Synthesis, Structure, Properties,and Applications* (Springer, 2001).
16. Baughman, R. H.; Zakhidov, A. A.; de Heer, W. A.,Carbon Nanotubes-the Route Toward Applications. *Science* 2002, 297, 787-792
17. Kim, B. Y. A.; Muramatsu, H.; Hayashi, T.; Endo, M.; Terrones, M.; Dresselhaus, M. S.,Fabrication of high purity, double-walled carbon nanotube buckypaper. *Chemical Vapor Deposition* 2006, 12, 327-330
18. Endo, M.; Muramatsu, H.; Hayashi, T.; Kim, Y. A.; Terrones, M.; Dresselhaus, M. S.,'Buckypaper' from coaxial nanotubes. *Nature* 2005, 433, 476
19. Zhang, X.; Sreekumar, T. V.; Liu, T.; Kumar, S.,Properties and Structure of Nitric Acis Oxidized Single Walled Carbon Nanotube Films. *Journal of Physical Chemistry B* 2004, 108, 16435-16440

20. Xu, G.; Zhang, Q.; Zhou, W.; Huang, J.; Wei, F.,The feasibility of producing MWCNT paper and strong MWCNT film from VACNT array. *Applied Physics A* 2008, 92, 531-539
21. Bandow, S.; Rao, A. M.; Williams, K. A.; Thess, A.; Smalley, R. E.; Eklund, P. C.,Purification of Single-Wall Carbon Nanotubes by Microfiltration. *Journal of Physical Chemistry B* 1997, 101, 8839-8842
22. Baughman, R. H.; Cui, C.; Zakhidov, A. A.; Iqbal, Z. B. J. N.; Spinks G. M.; Wallace, G. G.; Mazzoldi, A.; Rossi D. D.; Rinzler A. G.; Jaschinski, O.; Roth, S.; Kertesz, M.,Carbon Nanotube Actuators. *Science* 1999, 284, 1340-1344
23. Park, J. G.; Li, S.; Fan, X.; Zhang, C.; Wang, B.,The high current-carrying capacity of various carbon nanotube-based buckypapers. *Nanotechnology* 2008, 19, 185710-(1-7)
24. Park, T.-J.; Banerjee, S.; Hemraj-Benny, T.; Wong, S. S.,Purification strategies and purity visualization for single-walled carbon nanotubes. *J. Mater. Chem.* 2006, 16, 141-154
25. Suppiger, D.; Busato, S.; Ermanni, P.,Characterization of single-walled carbon nanotube mats and their performance as electromechanical actuators. *Carbon* 2008, 46, 1085-1090
26. Vohrer, U.; Kolaric, I.; Haque, M. H.; Roth, S.; Detlaff-Weglikowska, U.,Carbon nanotube sheets for the use as artificial muscles. *Carbon* 2004, 42, 1159-1164
27. Rouse, J. H.,Polymer-Assisted Dispersion of Single-Walled Carbon nanotubes in Alcohols and Applicability toward Carbon nanotube/Sol-Gel Composite Formation. *Langmuir* 2005, 21, 1055-1061
28. Cinke, M.; Li, J.; Chen, B.; Cassell, A.; Delzeit, L.; Han, J.; Meyyappan, M.,Pore structure of raw and purified HiPco single-walled carbon nanotubes. *Chem. Phys. Lett.* 2002, 365, 69-74
29. Dillon, A. C.; Gennett, T.; jones, K. M.; Alleman, J. L.; Parilla, P. A.; heben, M. J.,A simple and Complete Purification of Single-Walled Carbon nanotube Materials. *Advanced Materials* 1999, 11, 1354-1358
30. Xu, Y.-Q.; Peng, H.; Hauge, R. H.; Smalley, R. E.,Controlled Multistep Purification of Single-Walled Carbon Nanotubes. *Nano Letters* 2005, 5, 163-168
31. Ziegler, K. J.; Gu, Z.; Peng, H.; flor, E. L.; Hauge, R. H.; Smalley, R. E.,Controlled Oxidative Cutting of Single-Walled Carbon Nanotubes. *J. Am. Chem. Soc.* 2005 , 127, 1541-1547
32. Hu, H.; Zhao, B.; Itkis, M. E.; Haddon, R. C.,Nitric Acid Purification of single-Walled Carbon Nanotubes. *Journal of Physical Chemistry B* 2003, 107, 13838-13842
33. Bandow, S.; Asaka, S.; Zhao, X.; Ando, Y.,Purification and magnetic properties of carbon nanotubes. *Applied Physics A* 1998, 67, 23-27
34. Vaisman, L.; Wagner, H. D.; Marom, G.,The role of surfactants in dispersion of carbon nanotubes. *Adv. Colloid Interface Sci.* 2006, 128-130, 37-46
35. Sun, Z.; Nicolosi, V.; Rickard, D.; Bergin, S. D.; Aherne, D.; Coleman, J. N.,Quantitative Evaluation of Surfactant-stabilised Single-walled Carbon Nanotubes:Dispersion Quality and Its Corrleation with Zeta Potential. *Journal of Physical Chemistry C* 2008, 112, 10692-10699
36. Shaffer, M. S. P.; Fan, X.; Windle, A. H.,Dispersion and Packing of Carbon Nanotubes. *Carbon* 1998, 36, 1603-1612
37. Lin, T.; Bajapi, V.; Ji, T.; Dai, L.,Chemistry of Carbon Nanotubes. *Aust. J. Chem.* 2003, 56, 635-651

38. Yu, J.; Grossiord, N.; Koning, C. E.; Loos, J.,Controlling the dispersion of multi-wall carbon nanotubes in aqueous surfactant solution. *Carbon* 2007, 45, 618-623
39. Wang, Y.; Gao, L.; Sun, J.; Liu, Y.; Zheng, S.; Kajiura, H.; Li, Y.; Noda, K.,An integrated route for purification, cutting and dispersion of single-walled carbon nanotubes. *Chem. Phys. Lett.* 2006, 432, 205-208
40. Priya, B. R. and Byrne, H. J.,Investigation of Sodium Dodecyl Benzene Sulfonate Assisted Dispersion and Debundling of Single-Walled Carbon Nanotubes. *J. Phys. Chem.* 2008, 112, 332-337
41. Nish, A.; Hwang, J.-J.; Doig, J.; Nicholas, R. J.,Highly selective dispersion of single-walled carbon nanotubes using aromatic polymers. *Nature* 2007, 2, 640-646
42. Zheng, M.; Jagota, A.; Semke, E. D.; Diner, B. A.; Mclean, R. S.; Lustig, S. R.; Richardson, R. E.; Tassis, N. G.,DNA-assisted dispersion and separation of carbon nanotubes. *Nature* 2003, 2, 338-342
43. Hou, P.-X.; Liu, C.; Cheng, H.-M.,Purification of carbon nanotubes. *Carbon* 2008, 46, 2003-2025
44. Dumée, L.; Sears, K.; Schütz, J.; Finn, N.; Duke, M.; Gray., S.,Design and Characterisation of Carbon Nanotube Bucky-Paper Membranes for Membrane Distillation. *Desalination and Water Treatment* 2009, Submitted
45. Hernández, A. C. J. I.; Prádanos, P.; Tejerina, F. 1. 1. 1. p. p.,Pore size distributions in microporous membranes. A critical analysis of the bubble point extended method. *J. Membr. Sci.* 1996, 112, 1-12
46. Smajda, R.; Kukovecz, Á.; Kónya, Z.; Kiricsi, I.,Structure and gas permeability of multi-wall carbon nanotube buckypapers. *Carbon* 2007, 45, 1176-1184
47. Kukovecz, Á.; Smajda, R.; Kónya, Z.; Kiricsi, I.,Controlling the pore diameter distribution of multi-wall carbon nanotube buckypapers. *Carbon* 2007, 45, 1696-1716
48. Whitby, R. L. D.; Fukuda, T.; Maekawa, T.; James, S. L.; Mikhalovsky, S. V.,Geometric control and tuneable pore size distribution of buckypaper and buckydiscs. *Carbon* 2008, 46, 949-956
49. Das, R. K.; Liu, B.; Reynolds, J. R.; Rinzler, A. G.,Engineered Macroporosity in Single-Wall Carbon Nanotube Films. *Nano Letters* 2009, 9, 677-683
50. Casavant, M. J.; Walters, D. A.; Scmidt, J. J.; Smalley, R. E.,Neat macroscopic membranes of aligned carbon nanotubes. *J. Appl. Phys.* 2003, 93, 2153-2156
51. Wang, D.; Song, P.; Liu, C.; Wu, W.; Fan, S.,highly oriented carbon nanotube papers made of aligned carbon nanotubes. *Nanotechnology* 2008, 19, 075609(1-7)
52. Gonnet, P.; Liang, Z.; Choi, E. S.; Kadambala, R. S.; Zhang, C.; Brooks, J. S.; Wang, B.; Kramer, L.,Thermal conductivity of magnetically aligned carbon nanotube buckypapers and nanocomposites. *Current Applied Physics* 2006, 6, 119-122
53. Hone, J.; Liaguno, M. C.; nemes, N. M.; Johnson, A. T.; Fischer, J. E.; Walters, D. A.; Casavant, M. J.; Schmidt, J.; Smalley, R. E.,Electrical and thermal transport properties of magnetically aligned single wall carbon nanotube films. *Appl. Phys. Lett.* 2000, 77, 666-668
54. Lawson, K. W. and Lloyd, D. R.,Membrane distillation. *J. Membr. Sci.* 1997, 124, 1
55. Hoang, M.; Bolto, B.; Tran, T.,Desalination by Capacitive Deionisation. *Water* 2009, February 2009, 63-66

56. Pan, L.; Wang, X.; Zhang, Y.; Chen, Y.; Sun, Z.,Electrosorption of anions with carbon nanotube and nanofibre composite film electrodes. *Desalination* 2009, 244, 193-143
57. Wang, X.; Li, M.; Chen, R.; Huang, S.; Pan, L.; Sun, Z.,Electrosorption of ions from aqueous solutions with carbon nanotubes and nanofibers composite film electrodes. *Appl. Phys. Lett.* 2006, 89, 053127
58. Li, H.; Gao, Y.; Pan, L.; Zhang, Y. C. Y.; Sun, Z.,Electrosorptive desalination by carbon nanotubes and nanofibers electrodes and ion-exchange membranes. *Water Res.* 2008, 42, 4923-4928
59. Dai, K.; Shi, L.; Zhang, D. F. J.,NaCl adsorption in multi-walled carbon nanotube/active carbon combination electrode. *Chem. Eng. Sci.* 2006, 61, 428-433
60. Viswanathan, G.; Kane, D. B.; Lipowicz, P. J.,High efficiency fine particulate filtration using carbon nanotube coatings. *Advanced Materials* 2004, 16, 2045-2049
61. Kang, S.; Pinault, M.; Pfefferle, L. D.; Elimelech, M.,Single-Walled Carbon Nanotubes Exhibit Strong Antimicrobial Activity. *Langmuir* 2007, 23, 8670-8673
62. Brady-Esétvez, A. S.; Kang, S.; Elimelech, M.,A Single-Walled-Carbon-Nanotube Filter for Removal of Viral and Bacterial Pathogens. *Small* 2008, 4, 481-484
63. Hummer, G.; Rasalah, J. C.; Noworyta, J. P.,Water conduction through the hydrophobic channel of a carbon nanotube. *Nature* 2001, 414, 188-190
64. Skoulidas, A.; Ackerman, D. M.; Johnson, K.; Sholl, D. S.,Rapid transport of gases in carbon nanotubes. *Phys. Rev. Lett.* 2002, 89, 185901(1-4)
65. Chen, H.; Johnson, J. K.; Sholl, D. S.,Transport diffusion of gases is rapid in flexible carbon nanotubes. *Physical Chemistry B Letters* 2006, 110, 1971-1975
66. Waghe, A.; Rasaiah, J. C.; Hummer, G.,Filling and emptying kinetics of carbon nanotubes in water. *J. Chem. Phys.* 2002, 117, 10789-10795
67. Corry, B.,Designing Carbon Nanotube Membranes for Efficient Water Desalination. *Journal of Physical Chemistry B* 2008, 112, 1427-1434
68. Thomas, J. A. and McGaughey, J. H.,Reassessing Fast Water Transport Through Carbon Nanotubes. *Nano Letters* 2008, 8, 2788-2793
69. Zheng, J.; Lennon, E. M.; Tsao, H.-K.; Sheng, Y.-J.; Jiang, S.,Transport of a liquid water and methanol mixture through carbon nanotubes under a chemical gradient. *J. Chem. Phys.* 2005, 122, 214702 (1-7)
70. Striolo, A.,The mechanism of water diffusion in narrow carbon nanotubes. *Nanoletters* 2006, 6, 633-639
71. Majumder, S. R.; Choudhury, N.; Ghosh, S. K.,Enhanced flow in smooth single-file channel. *J. Chem. Phys.* 2007, 127, 054706 (1-5)
72. Allen, R.; Hansen, J.-P.; Melchionna, S.,Molecular dynamics investigation of water permeation through nanopores. *J. Chem. Phys.* 2003, 119, 3905-3919
73. Whitby, M. and Quirke, N.,Fluid flow in carbon nanotubes and nanopipes. *Nature* 2007, 2, 87-94
74. Sun, L. and Crooks, R.,Single Carbon Nanotube Membranes: A well-Defined Model for Studying Mass Transport through Nanoporous Materials. *Journal of American Chemical Society* 2000, 122, 12340-12345

75. Miller, S. and Martin, C.,Controlling the rate and direction of electroosmotic flow in template-prepared carbon nanotube membranes. *Journal of Electroanalytical Chemistry* 2002, 522, 66-69
76. Miller, S.; Young, V.; Marin, C.,Electroosmotic Flow in Template-Prepared Carbon Nanotube Membranes. *J. Am. Chem. Soc.* 2001, 123, 12335-12342
77. Naguib, N.; Ye, H.; Gogotsi, Y.; Yazicioglu, A. G.; Megaridis, C. M.; Yoshimura, M.,Observation of water confined in nanometer channels of closed carbon nanotubes. *Nanoletters* 2004, 4, 2237-2243
78. Rossi, M. P.; Ye, H.; Gogotsi, Y.; Babu, S.; Ndungu, P.; Bradley, J.-C.,Environmental Scanning Electron Microscopy Study of Water in Carbon Nanopipes. *Nano Letters* 2004, 4, 989-993
79. Majumder, M.; Chopra, N.; Hinds, B. J.,Effect of Tip Functionalization on Transport through Vertically Oriented Carbon Nanotube Membranes. *J. Am. Chem. Soc.* 2005, 127, 9062-9070
80. Nednoor, P. *et al.*,Reversible Biochemcial Switching of Ionic Transport through Aligned Carbon Nanotube Membranes. *Chemical Materials* 2005, 17, 3593-3599
81. Nednoor, P. *et al.*,Carbon nanotube based biomimetic membranes: mimicking protein channels regulated by phosphorylation. *J. Mater. Chem.* 17, 1755-1757
82. Majumder, M.; Zhan, X.; Andres, R.; Hinds, B. J.,Voltage gated carbon nanotube membranes. *Langmuir* 2007, 23, 8624-8631
83. Fornasiero, F. P. H. G.; Holt, J. K.; Stadermann, M.; Grigoropoulos, C. P.; Noy, A.; Bakajin, O.,Ion exclusion by sub-2-nm carbon nanotube pores. *Proceedings of the National Academy for Science* 2008, 0710437105 , 1-6
84. Sears, K.; Schütz, J.; Huynh, C.; Hawkins, S.; Humphries, W.,Evaluation and characterisation of carbon nanotube membranes. *Proceedings of the 2008 International Conference On Nanoscience and Nanotechnology (ICONN)* 2008, 37
85. Murakami, Y.; Chiashi, S.; Einarsson, E.; Maruyaman, S.,Polarization dependence of resonant Raman scattering from vertically aligned single-walled carbon nanotube films. *Physical Review B* 2005, 71, 085403 (1-8)
86. Duesberg, G. S.; Loa, I.; Burghard, M.; Syassen, K.; Roth, S.,Polarized Raman Spectroscopy on Isolated Single-Wall Carbon Nanotubes. *Phys. Rev. Lett.* 2000, 85, 5436-5439
87. Gommans, H. H.; Alldredge, J. W.; Tashiro, H.; Park, J.; Magnuson, J.,Fibers of aligned single-walled carbon nanoutbes: Polarized Raman spectroscopy. *J. Appl. Phys.* 2000, 88, 2509-2514
88. Yu, M.; Funke, H. H.; Falconer, J. L.; Noble, R. D.,High density, Vertically-Aligned Carbon Nanotube Membranes. *Nano Letters* 2009, 9, 225-229
89. Futaba, D. N.; Hata, K.; Yamada, T.; Hiraoka, T.; Hayamizu, Y.; Kakudate, Y.; Tanaike, O.; Hatori, H.; Yumura, M.; Iijima, S.,Shape-engineerable and highly densely packed single-walled carbon nanotubes and their application as super-capacitor electrodes. *Nature* 2006, 5, 987-994
90. Chakrapani, N.; Wei, B.; Carrillo, A.; Ajayan, P. M.; Kane, R. S.,Capillarity-driven assembly of two-dimensional cellular carbon nanotube foams. *Proceedings of the National Academy of Science* 2004, 101, 4009-4012
91. Jung, H. *et al.*,Anodic aluminum oxide membrane bonded on a silicon wafer for carbon nanotube field emitter arrays. *Appl. Phys. Lett.* 2006, 89, 013121-3
92. Onyestyák, Gy.; Valyon, J.; Hernádi, K.; kiricsi, I.; Rees, L. V. C.,Equilibrium and dynamics of acetylene sorption in multiwalled carbon nanotubes. *Carbon* 2003, 41, 1241-1248

93. Muramatsu, H.; Hayashi, T.; Kim, Y. A.; Shimamoto, D.; Kim, Y. J.; Tantrakarn, K.; Endo, M.; Terrones, M.; Dresselhaus, M. S.,Pore structure and oxidation stability of double-walled carbon nanotube-derived bucky paper. *Chem. Phys. Lett.* 2005, 414, 444-448
94. Inoue, S.; Ichikuni, N.; Suzuki, T.; Uematsu, T.; Kaneko, K.,Capillary Condensation of N2 on Multiwall Carbon Nanotubes. *The Journal of Physical Chemistry B* 1998, 102, 4689-4692
95. Cooper, S. M.; Chuang, H. F.; Cinke, M.; Cruden, B. A.; Meyyappan, M.,Gas permeability of a buckypaper membrane. *Nanoletters* 2003, 3, 189-192
96. Eswaramoorthy, M.; Sen, R.; Rao, C. N. R.,A study of micropores in single-walled carbon nanotubes by the adsorption of gases and vapors. *Chem. Phys. Lett.* 1999, 304, 207-210
97. Yang, C.-M.; Kaneko, K.; Yudasaka, M.; Iijima, S.,Effect of Purification on Pore Structure of HiPco Single-Walled Carbon nanotube Aggregates. *Nano Letters* 2002, 2, 385-388
98. Yang, C.-M.; Kim, D. Y.; lee, Y. H.,Formation of Densely Packed Single-Walled Carbon Nanotube assembly. *Chem. Mater.* 2005, 17, 6422-6429